JOURNAL OF GEOPHYSICAL RESEARCH, VOL. 114, C08005, doi:10.1029/2009JC005332, 2009

Statistics of nonlinear waves generated in an offshore wave basin

Z. Cherneva,[1] M. A. Tayfun,[2] and C. Guedes Soares[1]

Received 17 February 2009; revised 29 March 2009; accepted 10 April 2009; published 11 August 2009.

[1] This study analyzes waves generated in a deepwater wave basin and characterized by modulational instabilities induced by third-order nonlinear interactions among freely propagating waves, which can cause the statistics of various surface features to deviate significantly from the predictions based on the linear Gaussian and second-order models. Comparisons are provided between the statistics of wave envelopes and phases, wave heights, and crest and trough amplitudes observed for various theoretical approximations based on Gram-Charlier expansions. The results suggest that the comparisons for the wave envelopes tend to be somewhat poor, particularly in the presence of relatively strong instabilities. In contrast, the comparisons for wave phases, crest-to-trough heights, and crest and trough amplitudes all indicate that the theoretical approximations represent the empirical distributions observed reasonably well, for the most part. Furthermore, the heights and crests of the largest waves do not exceed Miche-Stokes-type upper bounds.

Citation: Cherneva, Z., M. A. Tayfun, and C. Guedes Soares (2009), Statistics of nonlinear waves generated in an offshore wave basin, *J. Geophys. Res.*, *114*, C08005, doi:10.1029/2009JC005332.

1. Introduction

[2] Relatively rare and unusually large oceanic waves, commonly referred to as abnormal, rogue or freak waves, have been the focus of intense research in recent years, aimed at understanding their physics and predicting under what conditions they are likely to occur. An obvious practical motivation for studying such waves is the potentially catastrophic damage risk which they pose for floating and fixed offshore or coastal structures. The term abnormal, rogue, or freak implies that the frequency of occurrence of such waves and the statistics describing their physical features significantly exceed the theoretical predictions based on the linear Gaussian or second-order statistical models [*Dean*, 1990; *Dysthe et al.*, 2008]. While most oceanic measurements indicate that a variety of linear Gaussian and second-order models describe the statistics of wave heights, crests and troughs observed quite accurately and consistently [*Tayfun and Fedele*, 2007a; *Tayfun*, 2008; *Fedele and Tayfun*, 2009; *Forristall*, 2007], some measurements occasionally contain one or two isolated outliers whose characteristics appear to noticeably exceed the trends predicted by the standard models [*Guedes Soares et al.*, 2003, 2004; *Petrova and Guedes Soares*, 2006; *Cherneva et al.*, 2008; *Tayfun*, 2008]. Whether such outliers represent typical occurrences in an atypical population of abnormal waves is a somewhat contentious issue [*Tayfun and Fedele*, 2007a; *Gemmrich and Garrett*, 2008; *Tayfun*, 2008; *Forristall*, 2005]. This is because although unusually large waves actually occur as relatively rare occurrences in a typical population of a large number of waves, as predicted by the standard statistical models, they can appear as outliers when viewed as samples within a smaller truncated segment of the same population [*Tayfun and Fedele*, 2007a]. This may be the case with outliers occasionally captured by 20-min measurements gathered intermittently at a fixed point of the sea surface [see, e.g., *Haver*, 2004].

[3] Quite a few recent studies explore if certain physical processes can generate freakish occurrences in a typical population of waves, such as the spatial focusing of waves due to refraction in variable bottom topography and/or currents [see, e.g., *Heller et al.*, 2008], dispersive focusing [*Kharif and Pelinovsky*, 2003] and nonlinear focusing, in particular, Benjamin-Feir (BF)-type modulational instabilities induced by third-order nonlinear interactions among free waves [*Onorato et al.*, 2001, 2006; *Janssen*, 2003; *Socquet-Juglard et al.*, 2005; *Mori et al.*, 2007; *Gramstad and Trulsen*, 2007]. These are all elaborated in a recent review [see *Dysthe et al.*, 2008, and references therein]. This study focuses only on the statistical effects of the third-order modulational instabilities, as predicted by the solutions of the Dysthe equation [*Dysthe*, 1979], a modified form of the nonlinear Schrödinger equation. It appears that the initial conditions conducive to the appearance of such instabilities require that waves be rather narrowband and long crested, which invariably lead to an abundance of abnormal wave occurrences in a typical population of numerically or mechanically generated waves as compared to just a few isolated outliers, if any at all, in oceanic measurements. Nevertheless, that actual populations of abnormal waves do in fact appear as a result of third-order instabilities has decisively been demonstrated in several laboratory experiments [see, e.g., *Stansberg*, 2000; *Onorato et al.*, 2006; *Shemer et al.*, 2007; *Shemer and Sergeeva*, 2009; *Petrova et al.*, 2008; *Petrova and Guedes Soares*,

[1]Centre for Marine Technology and Engineering, Instituto Superior Técnico, Technical University of Lisbon, Lisbon, Portugal.

[2]Department of Civil Engineering, College of Engineering and Petroleum, Kuwait University, Safat, Kuwait.

0148-0227/09/2009JC005332$09.00

2008], and also by way of the numerical solutions of the Dysthe and Euler equations [*Socquet-Juglard et al.*, 2005; *Toffoli et al.*, 2008].

[4] The present paper analyzes nonlinear waves generated in a large deepwater wave basin at Marintek in Trondheim, Norway in 1999, constructs the empirical distributions describing the wave envelopes and phases, wave heights, and crest and trough amplitudes observed, and compares these with several theoretical models recently proposed by *Tayfun and Fedele* [2007a] and *Tayfun* [2008]. The surface elevations measured at several gauges placed along the basin display third-order instabilities and contain an adequately large population of abnormal waves, rendering them amiable to statistical analyses and comparisons with the theoretical models.

[5] Similar experiments have been carried out at Marintek some years later [*Onorato et al.*, 2006; *Mori et al.*, 2007] and, more recently, in a large wave tank in Hanover, Germany [*Shemer et al.*, 2007; *Shemer and Sergeeva*, 2009]. Except for *Shemer and Sergeeva* [2009], all of these studies either focus on the statistics of wave heights and their comparisons with a theoretical approximation referred to as the modified Edgeworth-Rayleigh distribution [*Mori and Janssen*, 2006; *Mori et al.*, 2007; *Petrova et al.*, 2008; *Cherneva et al.*, 2008], or simply demonstrate how the observed wave heights, crests and toughs deviate from the linear and second-order predictions due to the BF-type modulational instabilities [*Onorato et al.*, 2006; *Toffoli et al.*, 2008].

[6] Only *Shemer and Sergeeva* [2009] consider comparisons of the theoretical models in *Tayfun and Fedele* [2007a] with the empirical statistics of the Hanover waves modulated by rather pronounced third-order instabilities. This study presents similar comparisons for the Marintek experiments. It also provides additional comparisons on wave envelopes and phases, and considers if the Miche-Stokes-type upper bounds have any relevance for the heights and crests of abnormal waves, thus exploring more comprehensively the relative validities of the theoretical approximations and conjectures proposed by *Tayfun and Fedele* [2007a] and *Tayfun* [2008].

2. Theoretical Distributions

[7] The theoretical expressions, which will be compared with the statistics of waves generated at the Marintek basin, represent approximations based on the Gram-Charlier (GC) expansions. The original application of such approximations to various surface features of a random seaway is due to *Longuet-Higgins* [1963]. The extensions to wave envelopes, phases, wave heights, and so on, not explored by Longuet-Higgins, were considered much later first by *Bitner* [1980], and then somewhat more systematically by *Tayfun and Lo* [1990] and *Tayfun* [1994], leading to several subsequent second- and third-order interpretations and applications in the work of *Mori and Janssen* [2006], *Tayfun and Fedele* [2007a], and *Tayfun* [2008].

[8] In this study, the comparisons with the Marintek data will draw on *Tayfun* [1994, 2008] and *Tayfun and Fedele* [2007a] because of the more general and comprehensive nature the theoretical expressions given in these references. Similarly, the analysis and relevance of the Miche-Stokes-type upper bounds to abnormal waves will also consider the formulations of *Tayfun* [2008].

2.1. Wave Envelopes and Phases

[9] Let η represent the nonlinear surface elevation from the mean water level, observed at a fixed point in time t. If the frequency spectrum of η and the associated simple moments are defined as $S(\omega)$ and m_j (j = 0, 1, ...), respectively, then $\sigma^2 = m_0$ is the variance of η, $\omega_m = m_1/m_0$ is the spectral central frequency, and $\nu = (m_0 m_2/m_1^2 - 1)^{1/2}$ is the spectral bandwidth. To define wave envelopes and phases, let $\hat{\eta}$ denote the Hilbert transform of η with respect to t. On this basis, the surface elevation can be rewritten as $\eta = \xi \cos \phi$, where $\xi(t) = (\eta^2 + \hat{\eta}^2)^{1/2}$ is the wave envelope and $\phi(t) = \tan^{-1}(\hat{\eta}/\eta)$ is the wave phase.

[10] Hereafter it will be assumed that η, $\hat{\eta}$, and thus ξ are all scaled with σ. In the presence of third-order nonlinearities, the exceedance distribution Q_ξ of ξ and the probability density p_ϕ of ϕ can be expressed in the approximate forms [*Tayfun and Fedele*, 2007a, 2008; *Tayfun*, 2008]

$$Q_\xi \equiv \Pr\{\xi > z\} = \exp\left(-z^2/2\right) \left[1 + \frac{\Lambda}{64} z^2\left(z^2 - 4\right)\right] \quad (1)$$

$$p_\phi = \frac{1}{2\pi}\left[1 - \frac{\lambda_{30}}{6}\sqrt{\frac{\pi}{2}}\cos\phi + \frac{\lambda_{40}}{24}\left(8\cos^4\phi - 12\cos^2\phi + 3\right) + \frac{\lambda_{22}}{4}\left(8\cos^2\phi\sin^2\phi - 1\right) + \frac{\lambda_{04}}{24}\left(8\sin^4\phi - 12\sin^2\phi + 3\right)\right], \quad (2)$$

where $\xi \geq 0$ by definition; $|\phi| < \pi$; $\lambda_{30} = \langle\eta^3\rangle$ is the skewness coefficient of η;

$$\lambda_{(4-n)n} \equiv \langle\eta^{4-n}\hat{\eta}^n\rangle + (-1)^{n/2}(3-n)(n-1), \quad (3)$$

for n = 0, 1, ..., 4, define the fourth-order joint normalized cumulants; and

$$\Lambda \equiv \lambda_{40} + 2\lambda_{22} + \lambda_{04}. \quad (4)$$

If third-order nonlinearities are negligible, then $\lambda_{(4-n)n} = O(\lambda_{30}^2) \approx 0$ typically, simplifying equations (1) and (2) to

$$Q_\xi \equiv Q_R(z) = \exp\left(-z^2/2\right) \quad (5)$$

$$p_\phi = \frac{1}{2\pi}\left(1 - \frac{\lambda_{30}}{6}\sqrt{\frac{\pi}{2}}\cos\varphi\right). \quad (6)$$

The first of these expressions, which is one of several possible forms associated with the Rayleigh exceedance distribution, describes wave envelopes in both linear and second-order waves. The second one approximates the wave-phase probability density in second-order waves and converges to the uniform probability density in linear waves where λ_{30} and all other third-order cumulants vanish.

[11] The explicit forms of the fourth-order cumulants are not known in the most general case. However, assume for a moment that $\lambda_{04} \rightarrow 3\lambda_{22} \rightarrow \lambda_{40}$ in the limit as $\nu \rightarrow 0$. As a result, $\Lambda \rightarrow \Lambda_{\text{app}} \equiv 8\lambda_{40}/3$ also, and equation (1) reduces to a form dependent only on λ_{40}, referred to as the modified Rayleigh-Edgeworth (MER) distribution by *Mori and Janssen* [2006]. Similarly, equation (2) converges to equation (6) identically [*Tayfun*, 2008]. Unfortunately, however, $\lambda_{40} > 3\lambda_{22} > \lambda_{04}$ and so $\Lambda_{\text{app}} > \Lambda$ invariably for all cases in the Marintek experiments, as will be seen shortly. So, the assumption that $\Lambda = \Lambda_{\text{app}} \equiv 8\lambda_{40}/3$ does not appear to be generally valid for waves characterized with third-order modulational instabilities. This study will therefore use the more general form of Λ given by equation (4) in all the theoretical expressions and their comparisons with the Marintek data, as in the work of *Shemer and Sergeeva* [2009].

2.2. Wave Heights

[12] Crest-to-trough wave heights depend on two-time statistics of the surface displacements or wave envelopes, as elaborated by *Boccotti* [1989] and *Tayfun* [1990], respectively [see also *Tayfun and Fedele*, 2007a]. Nearly all wave height models devised so far ignore this, and approximate the wave heights scaled with σ as $h \cong 2\xi$. Thus, the corresponding exceedance distribution is another form of the Rayleigh exceedance distribution, which follows by a simple change of variables from equation (5) as

$$Q_h(z) \cong Q_{2\xi}(z) = \exp\left(-z^2/8\right). \tag{7}$$

In general, $2\xi - h = O(\nu) > 0$ to the leading order of approximation [*Tayfun*, 1990]. Thus, substituting 2ξ for h overestimates the actual values of h. This is largely why comparisons with oceanic data and/or simulations often show that the Rayleigh exceedance distribution tends to overestimate the crest-to-trough heights of large waves by about 7%–8% [*Tayfun and Fedele*, 2007a].

[13] Wave heights are affected by nonlinearities, in particular, by the third-order modulational instabilities which tend to amplify λ_{40}, λ_{22}, and λ_{04} significantly above the trivial levels typical of second-order waves. An approximate exceedance distribution describing the scaled wave heights $h \cong 2\xi$ in such cases follows readily from equation (1) as

$$Q_{GC}(z) \cong Q_h(z)\left[1 + \frac{\Lambda}{1024}z^2\left(z^2 - 16\right)\right]. \tag{8}$$

2.3. Wave Crests and Troughs

[14] Clearly, $|\eta| \leq \xi$ by definition. Furthermore, linear wave crest and trough amplitudes scaled with σ are both given by $\xi - O(\nu/\xi)^2$. So, the Rayleigh exceedance distribution in equation (5) represents an upper bound and describes the crest and trough amplitudes in linear waves only if $\nu \rightarrow 0$ or as $\xi \rightarrow \infty$ asymptotically.

[15] In nonlinear waves, second-order harmonics introduce a vertical asymmetry to the surface profile, rendering wave crests sharper and higher, and troughs shallower and more rounded. This asymmetry does not appear to affect the statistics of wave heights significantly [*Tayfun and Fedele*, 2007a]. But, the exceedance distributions of crest and trough amplitudes do deviate from the Rayleigh form of equation (5) noticeably and tend to the following asymptotic forms, valid for relatively large waves in the most general case [*Tayfun and Fedele*, 2007a; *Fedele and Tayfun*, 2009]:

$$Q_{\xi^+}(z) = \Pr\{\xi^+ > z\} = \exp\left[-\frac{1}{2\mu^2}\left(-1 + \sqrt{1 + 2\mu z}\right)^2\right] \tag{9}$$

$$Q_{\xi^-}(z) = \Pr\{\xi^- > z\} = \exp\left[-\frac{1}{2}z^2\left(1 + \frac{1}{2}\mu z\right)^2\right], \tag{10}$$

where $\xi^+ = \xi(1 + \mu\xi/2) \geq \xi$ and $\xi^- = \xi(1 - \mu\xi/2) \leq \xi$ stand for the second-order crest and trough amplitudes, respectively, and μ represents a dimensionless measure of wave steepness. In the presence of third-order nonlinearities, the preceding expressions are modified further, assuming the approximate forms [*Tayfun and Fedele*, 2007a]

$$Q_{GC}^+(z) = Q_{\xi^+}(z)\left[1 + \frac{\Lambda}{64}z^2\left(z^2 - 4\right)\right] \tag{11}$$

$$Q_{GC}^-(z) = Q_{\xi^-}(z)\left[1 + \frac{\Lambda}{64}z^2\left(z^2 - 4\right)\right]. \tag{12}$$

The comparisons in *Shemer and Sergeeva* [2009] suggest that equation (8) and the preceding expressions represent the empirical data observed in the Hanover experiments reasonably well for the most part, but not with consistent quantitative accuracy in all cases.

[16] In theory, $\mu = \lambda_{30}/3$ exactly, provided that λ_{30} is derived from the directional spectrum of the "underlying" linear Gaussian surface [*Fedele and Tayfun*, 2009]. For relatively narrowband long-crested waves generated in the Marintek experiments, the values of μ estimated as $\langle\eta^3\rangle/3$ from the time series of surface elevations measured at different gauges as waves propagate along the basin do not significantly differ from one another or from the theoretical value $\mu = \lambda_{30}/3 \cong 0.075$ computed from the spectrum of the linear waves generated at the wave-maker.

[17] Using the Zakharov equation [*Zakharov*, 1999] as a starting point, *Fedele* [2008] derived a slightly different theoretical expression for the exceedance distribution of nonlinear wave crests. In the present notation, it is given by

$$Q_{GC}^+(z) = Q_{\xi^+}(z)\left[1 + \frac{\lambda_{40}}{24}z^2\left(z^2 - 3\right)\right]. \tag{13}$$

This expression is quite similar to equation (11), if one replaces Λ in the latter case with $\Lambda_{\text{app}} \equiv 8\lambda_{40}/3$. Not

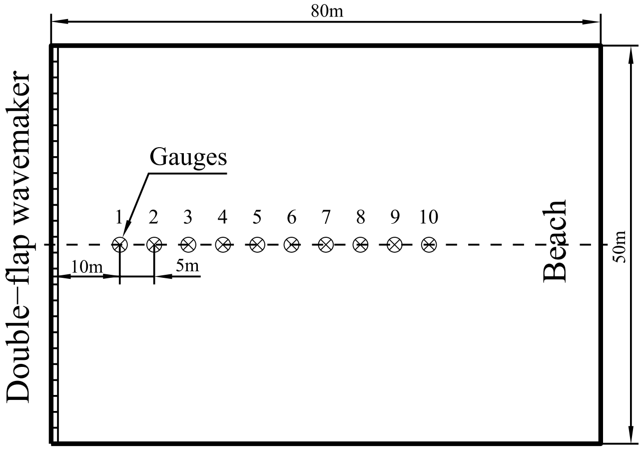

Figure 1. Layout of the Marintek wave basin and gauge locations.

surprisingly then, numerical comparisons of equations (11) and (13) here and in the work of *Fedele* [2008] for realistic values of the parameters μ and λ_{40} suggest that the two expressions are nearly the same whenever $\Lambda \approx \Lambda_{\mathrm{app}}$.

2.4. Upper Bounds to Wave Heights and Crests

[18] *Tayfun* [2008] assumes that an approximate upper bound to large wave heights is given by the Miche limit [*Miche*, 1944]

$$h_{\max} = \frac{2\pi}{7}\frac{\tanh kd}{\sigma k}, \tag{14}$$

where k is the wave number and d is the mean water depth. As $kd \to \infty$ in deep water, equation (14) converges to the Stokes limit. As a first order of approximation, $h_{\max}$ can be substituted in *Boccotti*'s [1989] quasideterministic model for large waves to obtain an upper bound to wave crests in the form

$$\xi^{+}_{\max 1} = \frac{h_{\max}}{1-a}, \tag{15}$$

where a represents the first minimum of $\rho(\tau) \equiv \langle \eta(t)\eta(t+\tau)\rangle$. In general, $-1 \le a < 0$ such that $a \to -1$ in the limit as $\nu \to 0$. For the JONSWAP spectrum simulated at the wave-maker, $a \cong -0.727$.

[19] As a higher order of approximation, $\xi^{+}_{\max\ 1}$ can also be coupled with the general second-order representation of large wave crests [*Fedele and Tayfun*, 2009], leading to a somewhat more conservative upper bound given by

$$\xi^{+}_{\max 2} = \xi^{+}_{\max 1}\left(1 + \frac{1}{2}\mu\xi^{+}_{\max 1}\right). \tag{16}$$

The comparisons with oceanic data confirm the validity of the preceding upper bounds [*Tayfun*, 2008]. Whether they have any relevance in waves characterized with third-order modulational instabilities would be of practical value since the existence of such bounds makes it possible to estimate quite reliably not only the maximum wave height and crest possible in a sea state, but also the expected shape of the largest wave and associated dynamics in time and space, given the spectrum of the sea surface [*Tayfun and Fedele*, 2007b, 2008; *Fedele and Tayfun*, 2009].

3. Experimental Data

[20] The data to be analyzed and compared with the preceding theoretical expressions were obtained during a sequence of five experiments run in a fairly large deepwater wave basin at Marintek in 1999. Figure 1 shows the layout of the basin and the locations of the capacitance wave gauges used for measuring the water surface elevations. The first gauge is at 10 m from a double-flap wave-maker, and the subsequent gauges are placed at a uniform spacing of 5 m along the section where the water depth is 2 m. A sloping beach at the end of the basin serves to absorb the incident wave energy.

[21] The length scale of the experiments is 1:50. At the wave-maker, linear waves are generated as sums of independent Gaussian wave components with Rayleigh-distributed amplitudes and uniformly random phases. Each experiment uses different sets of random phases and amplitudes, but the variance of amplitudes is such that the spectrum of waves generated at the wave-maker mimic at full scale a truncated JONSWAP spectrum characterized with the Phillips parameter $\alpha \cong 0.0178$, peak enhancement factor $\gamma = 3$, peak frequency $\omega_{\mathrm{p}} = 0.897$ rad s^{-1}, and it is band-limited to frequencies in $(0, 3\omega_{\mathrm{p}})$. So, for the full-scale waves generated at the wave-maker, $\sigma = 0.875$ m, $T_{\mathrm{p}} = 2\pi/\omega_{\mathrm{p}} = 7$ s, $\nu = 0.298$, $k_{\mathrm{p}} = \omega_{\mathrm{p}}^2/g = 0.082$ m^{-1} and steepness $s_{\mathrm{p}} = \sigma\ k_{\mathrm{p}} = 0.072$. All these change somewhat as waves propagate along the basin in the manner illustrated in Table 1, summarizing the ensemble averages from five experimental series observed at gauges 1–10. Statistical tests do not reject the hypothesis that all five experimental series observed at a given gauge have the same mean and variance [cf. *Petrova and Guedes Soares*, 2006].

[22] The duration of each experiment is 3.17 h at full scale. A typical 3.17-h surface elevation series gathered at a uniform sampling rate of 5.66 Hz contains about 1800 waves. Thus, the statistics and comparisons to follow will be based on an ensemble of five similar but independent series collected from the same gauge, comprising about 9000 waves altogether.

[23] Table 2 summarizes all the nontrivial third- and fourth-order ensemble-averaged cumulants required by the theoretical expressions. It is evident that as waves propagate along the basin, third-order modulational instabilities tend

Table 1. Principal Parameters Observed at Gauges 1–10

Gauge	σ (m)	T_{p} (s)	k_{p} (m^{-1})	μ	ν
1	0.935	6.963	0.083	0.073	0.298
2	0.914	6.963	0.083	0.077	0.293
3	0.901	6.963	0.083	0.074	0.285
4	0.875	6.963	0.083	0.072	0.282
5	0.838	6.963	0.083	0.073	0.284
6	0.824	7.079	0.081	0.076	0.284
7	0.819	7.079	0.081	0.075	0.275
8	0.813	7.079	0.081	0.073	0.273
9	0.819	7.311	0.076	0.073	0.271
10	0.809	7.195	0.078	0.071	0.268

Table 2. Nontrivial Cumulants λ_{mn}, Λ, and Λ_{app}/Λ Observed at Gauges 1–10

Gauge	λ_{30}	λ_{12}	λ_{40}	λ_{22}	λ_{04}	Λ	Λ_{app}/Λ
1	0.218	0.073	0.261	0.071	0.163	0.566	1.230
2	0.231	0.077	0.397	0.110	0.265	0.882	1.200
3	0.221	0.074	0.473	0.133	0.325	1.064	1.185
4	0.216	0.072	0.525	0.154	0.399	1.232	1.136
5	0.219	0.073	0.682	0.200	0.520	1.602	1.135
6	0.227	0.076	0.673	0.206	0.565	1.650	1.088
7	0.225	0.075	0.680	0.204	0.542	1.630	1.112
8	0.218	0.073	0.731	0.221	0.597	1.770	1.101
9	0.218	0.073	0.678	0.201	0.528	1.608	1.124
10	0.214	0.071	0.663	0.200	0.536	1.599	1.106

to increase, as reflected by the progressively larger Λ values observed, starting with 0.566 at gauge 1 and reaching a peak of 1.770 at gauge 8.

[24] Interestingly, $\lambda_{30} = 3\lambda_{12}$ almost exactly in all cases, as for second-order nonlinear waves [cf. *Tayfun and Lo*, 1990; *Tayfun*, 1994]. Furthermore, λ_{21}, λ_{03}, λ_{31}, and λ_{13} not shown in Table 2 are essentially zero, apparently confirming previous theoretical results on second- and third-order waves [*Tayfun and Lo*, 1990; *Tayfun*, 1994; *Mori and Janssen*, 2006; *Tayfun*, 2008].

[25] However, the comparisons of $\Lambda = \lambda_{40} + 2\lambda_{22} + \lambda_{04}$ and $\Lambda_{app} = 8\lambda_{40}/3$ indicate that $\Lambda_{app} > \Lambda$ in all cases, as mentioned before.

4. Comparisons With Theoretical Predictions

[26] For economy of space, the comparisons here will focus only on the measurements at gauges 1, 5, and 8 where the modulational instabilities appear to be at their initial, intermediate and peak stages of development. Also, for clarity in graphics, the statistics observed at these gauges will be compared with the predictions based for the most part on the third-order GC approximations, represented by equations (1) and (2) for wave envelopes and phases, (8) for wave heights, and equations (11) and (12) for wave crest and trough amplitudes, respectively. For contrast, the comparisons will also include the Rayleigh limits described by equations (5) and (7) for linear and second-order wave envelopes and wave heights, and also equation (6) for wave phases. Equations (9) and (10) for second-order wave crests and troughs are not considered here, again for clarity of graphical presentations and also not to repeat several similar comparisons elaborated elsewhere [see, e.g., *Socquet-Juglard et al.*, 2005; *Onorato et al.*, 2006; *Toffoli et al.*, 2008; *Shemer and Sergeeva*, 2009].

[27] As shown in Figure 2, the comparisons between the wave envelope exceedance distributions observed and the predictions from equation (1) do not appear generally favorable, except for the comparisons at gauge 1 where the third-order modulations have not yet fully developed to affect the surface features more significantly than the second-order nonlinear effects. This view changes rather noticeably at gauge 5 and particularly at gauge 8 where the modulational instabilities seem to have fully developed, causing the empirical data to significantly exceed the theoretical predictions over relatively large waves.

[28] The comparisons of the wave-phase probability densities observed with the predictions from equations (2) and (6) are shown in Figure 3. Although the theoretical predictions are not entirely impressive in terms of their quantitative accuracy, they seem to represent the empirical trends reasonably well and clearly far better than the uniform probability density appropriate to linear waves. It is seen that equation (2) compares somewhat better with the

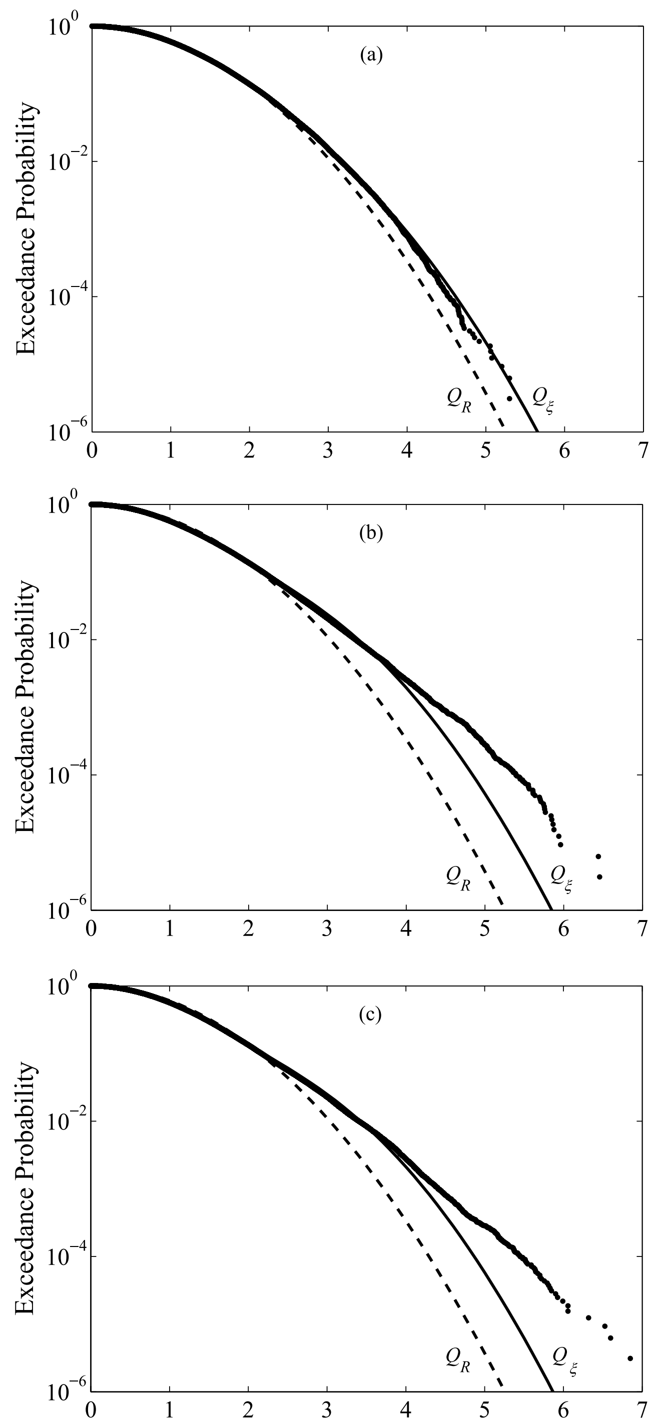

Figure 2. Wave envelope exceedance distributions: Marintek data (points) compared to third-order Gram-Charlier (GC) predictions (Q_ξ) from equation (1) and Rayleigh predictions (Q_R) from equation (5), valid for linear and second-order wave envelopes at (a) gauge 1, (b) gauge 5, and (c) gauge 8.

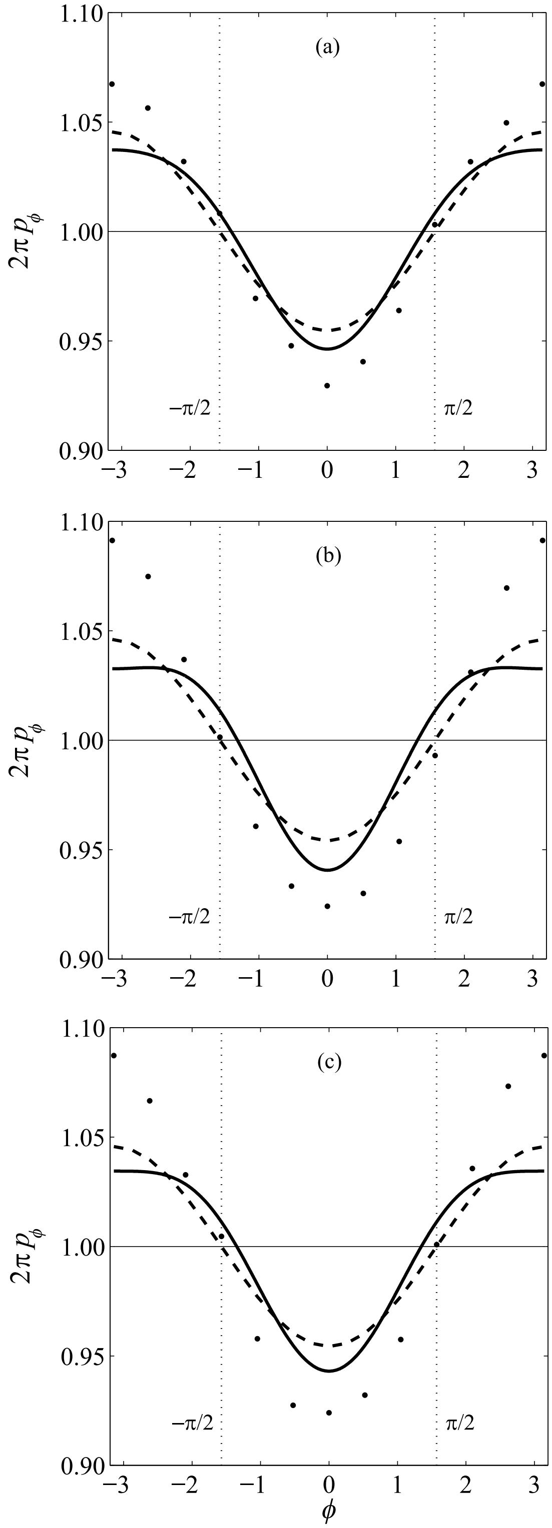

Figure 3. Wave phase probability densities: Marintek data (solid circles) compared to the theoretical uniform probability density (straight horizontal lines) valid for linear waves, third-order probability density (continuous curves) from equation (2), and the second-order probability density (dashed curves) from equation (6) at (a) gauge 1, (b) gauge 5, and (c) gauge 8.

phases over wave crests where $|\phi| < \pi/2$ whereas equation (6) does relatively better over the wave troughs even though it is not, strictly speaking, a theoretically valid model in these comparisons since $\Lambda_{app} \neq \Lambda$.

[29] Figure 4 shows the comparisons of the empirical exceedance distributions of crest-to-trough wave heights, and crest and trough amplitudes with the third-order GC predictions and the linear Rayleigh limits. The predictions seem to agree reasonably well with the experimental data, except for the wave heights observed at gauge 1 where $\Lambda < 1$. Otherwise, the general nature of the results in this figure is fairly similar to those of *Shemer and Sergeeva* [2009].

[30] Figure 5 shows the scatter diagrams of 50 wave heights and crests, each of which represents the largest in a 3.17-h surface series collected at a gauge, and the associated zero upcrossing periods T scaled with T_p in comparisons with the upper limits predicted from equations (14)–(16) with $d = 100$ m, $a \cong -0.727$, and $\sigma = 0.855$ m, $T_p = 7.056$ s and $\mu = 0.074$ representing the averages of the values in Table 1. These comparisons clearly confirm the relative validity of the Miche-Stokes-type upper bounds, namely h_{max} to wave heights and $\xi^+_{max\ 2}$ to wave crests, as in previous comparisons with oceanic data [*Tayfun and Fedele*, 2008; *Tayfun*, 2008].

5. Discussion and Conclusions

[31] Third-order GC approximations describing the statistics of wave heights and envelopes critically depend on a single dimensionless parameter, Λ, requiring the even fourth-order joints cumulants of the surface elevation and its Hilbert transform. The corresponding GC approximations for wave phases, and crest and trough amplitudes depend in addition on the skewness coefficient λ_{30}. In general, Λ reflects the relative importance of symmetric amplifications induced by third-order modulational instabilities whereas λ_{30} is a measure of the vertical asymmetry of the free surface largely due to second-order bound waves.

[32] The comparisons with the Marintek data suggest that the quantitative accuracy of the third-order GC approximations is not assured in all cases. This is particularly so for the wave envelopes observed at gauges 5 and 8, where the GC approximations consistently under predict the actual envelopes over large waves. Instabilities are rather pronounced at gauges 5 and 8, but not so at gauge 1 where, as a result, the GC approximation does quite well. In essence, a similar conclusion is also valid for the wave-phase comparisons. It appears then that the quantitative accuracy of GC approximations in representing the statistics of wave envelopes and phases is not impressive if $\Lambda > 1$ approximately. In contrast, the GC predictions for the wave heights, crests, and trough amplitudes observed suggest just the opposite in that they compare reasonably well with the actual statistics observed at gauges 5 and 8 where $\Lambda > 1$, but do relatively poorly at guage 1 where modulational instabilities have not yet developed fully.

[33] As in previous similar comparisons with oceanic waves, the heights and crests of the largest waves observed in these particular experiments do not exceed the Miche-Stokes-type upper bounds either. The existence of such bounds has significance both theoretically and practically since it makes it possible to estimate not only the maximum

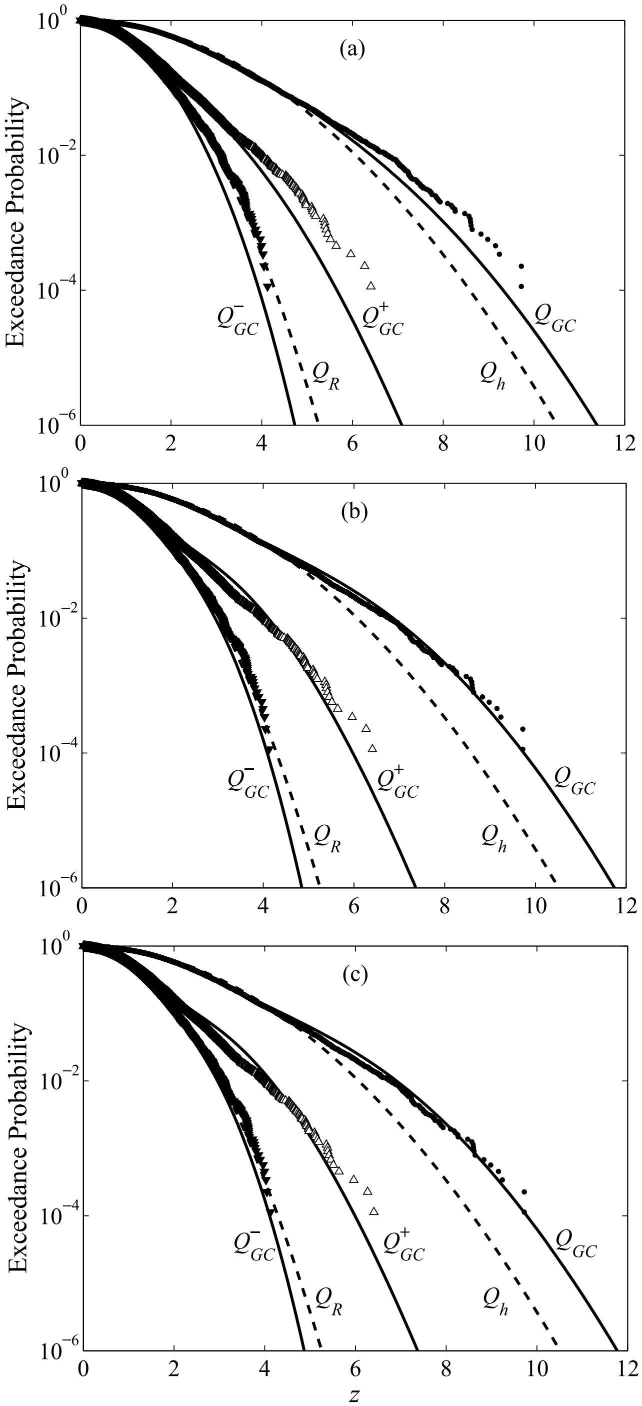

Figure 4. The empirical exceedance distributions describing crest-to-trough wave heights (points), crests (open triangles), and trough amplitudes (solid triangles) observed at (a) gauge 1 (9126 waves), (b) gauge 5 (8907 waves), and (c) gauge 8 (8819 waves) compared to the third-order GC approximations Q_{GC} (equation (8)) for wave heights, Q^+_{GC} (equation (11)) for wave crests, Q^-_{GC} (equation (12)) for trough amplitudes, and the Rayleigh limits Q_h (equation (7)) for linear wave heights and Q_R (equation (5)) for linear crests and trough amplitudes.

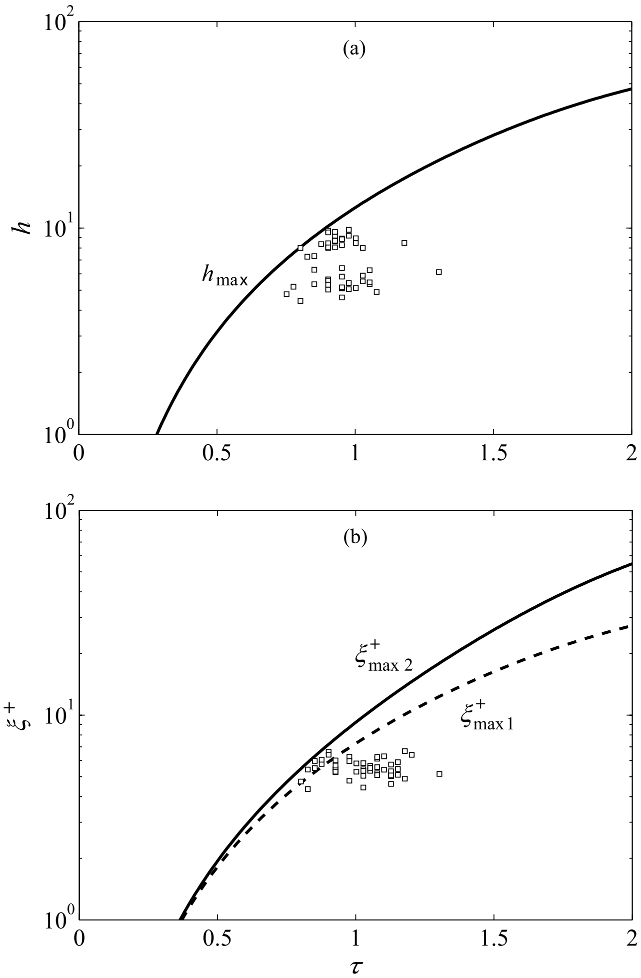

Figure 5. The scatter diagrams of the largest wave heights and wave crests: (a) the largest 50 crest-to-trough wave heights h and associated zero upcrossing wave periods $\tau = T/T_p$ observed at gauges 1–10 compared to the Miche-Stokes upper limit of equation (14) and (b) the largest 50 wave crests ξ^+ and associated zero upcrossing wave periods τ observed at gauges 1–10 compared to the upper limits $\xi^+_{\max\ 1}$ and $\xi^+_{\max\ 2}$ from equations (15) and (16), respectively.

wave height and crest possible in a sea state, but also the expected shape of the largest wave and associated dynamics in time and space, given the spectrum of the sea surface. These will be explored further in a future study.

[34] **Acknowledgments.** The first author was supported by the Portuguese Foundation for Science and Technology with grant SFRH/BRD/30589/2006. The data were obtained by the third author at Marintek, Trondheim, in 1999 as a part of the project Interactions Between Waves and Currents, partially funded by the European Union under contract ERBFMGECT980135 for access to large-scale facilities.

References

Bitner, E. (1980), Nonlinear effects of the statistical model of shallow-water wind waves, *Appl. Ocean Res.*, *2*, 63–73, doi:10.1016/0141-1187(80)90031-0.

Boccotti, P. (1989), *On mechanics of irregular gravity waves*, *Atti Accademia Nazionale Lincei, Memorie VIII*, *19*, 111–170.

Cherneva, Z., C. Guedes Soares, and P. Petrova (2008), Distribution wave height maxima in storm sea states, in *2008 Proceedings of the ASME 27th International Conference on Offshore Mechanics and*

Arctic Engineering, [CD-ROM], paper OMAE2008-58038, Am. Soc. of Mech. Eng., New York.
Dean, R. (1990), Abnormal waves: A possible explanation, in *Water Wave Kinematics*, edited by A. Torum and O. Gudmestat, pp. 609–612, Kluwer, New York.
Dysthe, K. (1979), Note on a modification to the nonlinear Schrödinger equation for application to deep water waves, *Proc. R. Soc. London, Ser. A*, *369*, 105–114, doi:10.1098/rspa.1979.0154.
Dysthe, K., H. Krogstad, and P. Müller (2008), Oceanic rogue waves, *Annu. Rev. Fluid Mech.*, *40*, 287–310, doi:10.1146/annurev.fluid.40.111406.102203.
Fedele, F. (2008), Rogue waves in oceanic turbulence, *Physica D*, *237*, 2127–2131, doi:10.1016/j.physd.2008.01.022.
Fedele, F., and M. A. Tayfun (2009), On nonlinear wave groups and crest statistics, *J. Fluid Mech.*, *620*, 221–239, doi:10.1017/S0022112008004424.
Forristall, G. (2005), Understanding rogue waves: Are new physics really necessary?, paper presented at 14th 'Aha Huliko'a Hawaiian Winter Workshop, U.S. Off. of Nav. Res., Honolulu, Hawaii, 25–28 Jan.
Forristall, G. (2007), Comparing hindcasts with measurements from hurricanes Lili, Ivan, and Katrina, paper presented at the 10th International Workshop on Wave Hindcasting and Forecasting and Coastal Hazard Symposium, Coastal and Hydraul. Lab., U.S. Army Eng. Res. and Dev. Cent., Oahu, Hawaii, 11–16 Nov.
Gemmrich, J., and C. Garrett (2008), Unexpected waves, *J. Phys. Oceanogr.*, *38*, 2330–2336, doi:10.1175/2008JPO3960.1.
Gramstad, O., and K. Trulsen (2007), Influence of crest and group length on the occurrence of freak waves, *J. Fluid Mech.*, *582*, 463–472, doi:10.1017/S0022112007006507.
Guedes Soares, C., Z. Cherneva, and E. Antão (2003), Characteristics of abnormal waves in North Sea storm sea states, *Appl. Ocean Res.*, *25*, 337–344, doi:10.1016/j.apor.2004.02.005.
Guedes Soares, C., Z. Cherneva, and E. M. Antão (2004), Abnormal waves during hurricane Camille, *J. Geophys. Res.*, *109*, C08008, doi:10.1029/2003JC002244.
Haver, S. (2004), A possible freak wave event measured at the Draupner Jacket January 1 1995, in *Rogue Waves 2004*, edited by M. Olagnon and M. Prevosto, Inst. Fr. de Rech. pour l'Exploit. de la Mer (Ifremer), Brest, France.
Heller, E. J., L. Kaplan, and A. Dahlen (2008), Refraction of a Gaussian seaway, *J. Geophys. Res.*, *113*, C09023, doi:10.1029/2008JC004748.
Janssen, P. A. E. M. (2003), Nonlinear four-wave interactions and freak waves, *J. Phys. Oceanogr.*, *33*, 863–884, doi:10.1175/1520-0485(2003)33<863:NFIAFW>2.0.CO;2.
Kharif, C., and E. Pelinovsky (2003), Physical mechanisms of the rogue wave phenomenon, *Eur. J. Mech. B*, *22*, 603–634, doi:10.1016/j.euromechflu.2003.09.002.
Longuet-Higgins, M. S. (1963), The effect of nonlinearities on statistical distributions in the theory of sea waves, *J. Fluid Mech.*, *17*, 459–480, doi:10.1017/S0022112063001452.
Miche, R. (1944), Mouvements ondulatoires de la mer en profoundeur constante ou Decroissante, *Ann. Ponts Chaussees*, *121*, 285–318.
Mori, N., and P. A. E. M. Janssen (2006), On kurtosis and occurrence probability of freak waves, *J. Phys. Oceanogr.*, *36*, 1471–1483, doi:10.1175/JPO2922.1.
Mori, N., M. Onorato, A. E. M. P.Janssen, A. Osborne, and M. Serio (2007), On the extreme statistics of long-crested deep water waves: Theory and experiments, *J. Geophys. Res.*, *112*, C09011, doi:10.1029/2006JC004024.
Onorato, M., A. R. Osborne, M. Serio, and S. Bertone (2001), Freak waves in random oceanic sea states, *Phys. Rev. Lett.*, *86*, 5831–5834, doi:10.1103/PhysRevLett.86.5831.
Onorato, M., A. R. Osborne, M. Serio, L. Cavaleri, C. Brandini, and C. Stansberg (2006), Extreme waves, modulational instability and second order theory: Wave flume experiments on irregular waves, *Eur. J. Mech. B*, *25*, 586–601, doi:10.1016/j.euromechflu.2006.01.002.
Petrova, P., and C. Guedes Soares (2006), Spatial variability of the wave field generated in an offshore basin, in *STAB2006: 9th International Conference on Stability of Ships and Ocean Vehicles*, edited by M. Neves, pp. 287–298, COPPE/UFRJ, Rio de Janeiro, Brazil.
Petrova, P., and C. Guedes Soares (2008), Maximum wave crest and height statistics of irregular and abnormal waves in an offshore basin, *Appl. Ocean Res.*, *30*, 144–152, doi:10.1016/j.apor.2008.08.004.
Petrova, P., C. Guedes Soares, and Z. Cherneva (2008), Influence of the third order nonlinearity on the distribution of wave height maxima in an offshore basin, in *2008 Proceedings of the ASME 27th International Conference on Offshore Mechanics and Arctic Engineering*, [CD-ROM], paper OMAE2008-58049, Am. Soc. of Mech. Eng., New York.
Shemer, L., and A. Sergeeva (2009), An experimental study of spatial evolution of statistical parameters in a unidirectional narrow-banded random wave field, *J. Geophys. Res.*, *114*, C01015, doi:10.1029/2008JC005077.
Shemer, L., K. Goulitski, and E. Kit (2007), Evolution of wide-spectrum wave groups in a tank: An experimental and numerical study, *Eur. J. Mech. B*, *26*, 193–219, doi:10.1016/j.euromechflu.2006.06.004.
Socquet-Juglard, H., K. Dysthe, K. Trulsen, H. Krogstad, and J. Liu (2005), Probability distributions of surface gravity waves during spectral changes, *J. Fluid Mech.*, *542*, 195–216, doi:10.1017/S0022112005006312.
Stansberg, C. (2000), Nonlinear extreme wave evolution in random wave groups, *Proceedings of the 10th ISOPE Conference*, *III*, 1–8, Int. Soc. of Offshore and Polar Eng., Cupertino, Calif.
Tayfun, M. A. (1990), Distribution of large wave heights, *J. Waterw. Port Coastal Ocean Eng.*, *116*, 686–707, doi:10.1061/(ASCE)0733-950X(1990)116:6(686).
Tayfun, M. A. (1994), Distributions of wave envelope and phase in weakly nonlinear random waves, *J. Eng. Mech.*, *120*, 1009–1025, doi:10.1061/(ASCE)0733-9399(1994)120:5(1009).
Tayfun, M. A. (2008), Distributions of envelope and phase in wind waves, *J. Phys. Oceanogr.*, *38*, 2784–2800, doi:10.1175/2008JPO4008.1.
Tayfun, M. A., and F. Fedele (2007a), Wave-height distributions and nonlinear effects, *Ocean Eng.*, *34*, 1631–1649, doi:10.1016/j.oceaneng.2006.11.006.
Tayfun, M. A., and F. Fedele (2007b), Expected shape of extreme waves in storm seas, in *2008 Proceedings of the ASME 27th International Conference on Offshore Mechanics and Arctic Engineering*, [CD-ROM], paper OMAE2007-29073, Am. Soc. of Mech. Eng., New York.
Tayfun, M. A., and F. Fedele (2008), Envelope and phase statistics of large waves, in *2008 Proceedings of the ASME 27th International Conference on Offshore Mechanics and Arctic Engineering*, [CD-ROM], paper OMAE2008-57,129, Am. Soc. of Mech. Eng., New York.
Tayfun, M. A., and J.-M. Lo (1990), Non-linear effects on wave envelope and phase, *J. Waterw. Port Coastal Ocean Eng.*, *116*, 79–100, doi:10.1061/(ASCE)0733-950X(1990)116:1(79).
Toffoli, A., E. Bitner-Gregersen, M. Onorato, A. R. Osborne, and A. V. Babanin (2008), Surface gravity waves from direct numerical simulations of the Euler equations: A comparison with second-order theory, *Ocean Eng.*, *35*, 367–379, doi:10.1016/j.oceaneng.2007.10.004.
Zakharov, V. E. (1999), Statistical theory of gravity and capillary waves on the surface of a finite-depth fluid, *Eur. J. Mech. B*, *18*, 327–344, doi:10.1016/S0997-7546(99)80031-4.

Z. Cherneva and C. Guedes Soares, Centre for Marine Technology and Engineering, Instituto Superior Técnico, Technical University of Lisbon, Av. Rovisco Pais, P-1049-001, Lisbon, Portugal. (guedess@mar.ist.utl.pt)

M. A. Tayfun, Department of Civil Engineering, College of Engineering and Petroleum, Kuwait University, P.O. Box 5969, 13060 Safat, Kuwait.